

Effects of PEG-Linker Chain Length of Folate-Linked Liposomal Formulations on Targeting Ability and Antitumor Activity of Encapsulated Drug

Chaemin Lim^{1,*}, Yuseon Shin^{2,*}, Kioh Kang², Patihul Husni², Dayoon Lee², Sehwa Lee², Han-Gon Choi³, Eun Seong Lee⁴, Yu Seok Youn⁵, Kyung Taek Oh^{1,2}

¹College of Pharmacy, Chung-Ang University, Seoul, 06974, Republic of Korea; ²Department of Global Innovative Drugs, The Graduate School of Chung-Ang University, Seoul, 06974, Republic of Korea; ³College of Pharmacy, Hanyang University, Ansan, 15588, South Korea; ⁴Department of Biotechnology, The Catholic University of Korea, Bucheon-si, Gyeonggi-do, 14662, Republic of Korea; ⁵School of Pharmacy, Sungkyunkwan University, Suwon, Gyeonggi-do, 16419, Republic of Korea

*These authors contributed equally to this work

Correspondence: Kyung Taek Oh, College of Pharmacy, Chung-Ang University, 221 Heukseok-dong, Dongjak-gu, Seoul, 06974, Republic of Korea, Tel +82-2-824-5617, Email kyungoh@cau.ac.kr

Introduction: Ligand-conjugated liposomes are promising for the treatment of specific receptor-overexpressing cancers. However, previous studies have shown inconsistent results because of the varying properties of the ligand, presence of a polyethylene glycol (PEG) coating on the liposome, length of the linker, and density of the ligand.

Methods: Here, we prepared PEGylated liposomes using PEG-linkers of various lengths conjugated with folate and evaluated the effect of the PEG-linker length on the nanoparticle distribution and pharmacological efficacy of the encapsulated drug both in vitro and in vivo.

Results: When folate was conjugated to the liposome surface, the cellular uptake efficiency in folate receptor overexpressed KB cells dramatically increased compared to that of the normal liposome. However, when comparing the effect of the PEG-linker length in vitro, no significant difference between the formulations was observed. In contrast, the level of tumor accumulation of particles in vivo significantly increased when the length of the PEG-linker was increased. The tumor size was reduced by >40% in the Dox/FL-10K-treated group compared to that in the Dox/FL-2K- or 5K-treated groups.

Discussion: Our study suggests that as the length of PEG-linker increases, the tumor-targeting ability can be enhanced under in vivo conditions, which can lead to an increase in the antitumor activity of the encapsulated drug.

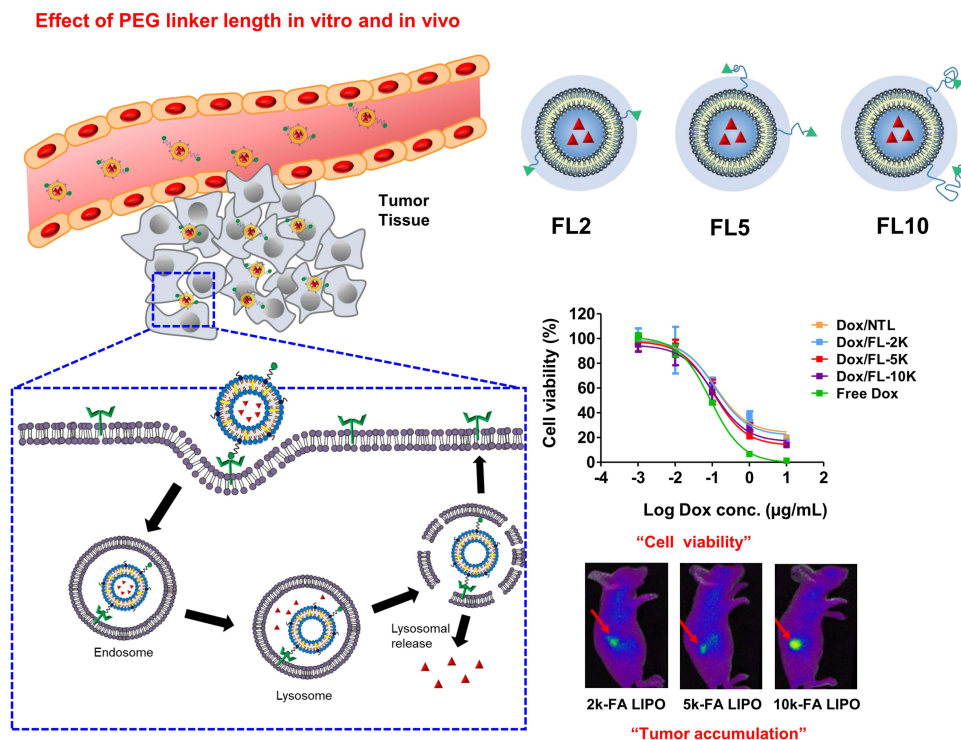
Keywords: PEGylated liposome, ligand-conjugated liposome, folate receptor, PEG-linker length

Introduction

Use of nanotechnology in cancer treatment has gained considerable interest in recent times for drug delivery.¹⁻⁴ Numerous researchers have employed nanotechnology to improve drug bioavailability and mitigate the toxicity and adverse effects associated with drugs.⁵⁻⁷ In particular, various types of nano-sized drug-delivery systems, such as liposomes, nanogels, polymeric micelles, and lipid nanoparticles, have been developed to maximize drug efficacy by controlling drug release from tumor tissues.⁸⁻¹²

Liposomes are the most commonly used drug-delivery systems.¹³⁻¹⁸ They can encapsulate both hydrophilic and hydrophobic molecules and improve cellular uptake at the tumor site owing to enhanced permeability and retention (EPR). When liposomes are pegylated, they are often referred to as “stealth carriers” because the PEG coating reduces their recognition and clearance by the immune system.¹⁹⁻²¹ Compared to small molecules, the liposome system offers

Graphical Abstract

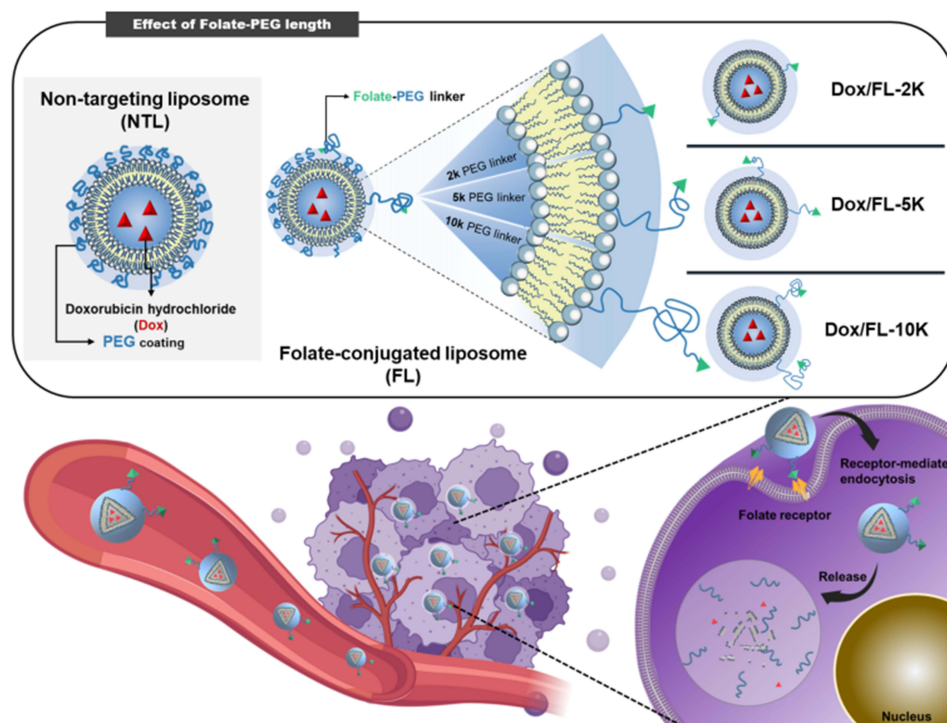


various advantages such as self-assembly, biocompatibility, and favorable physicochemical properties that can change the properties of drugs.^{15,22} An important feature of liposomes is that various functional groups can be introduced on their surfaces that provide an attractive scaffold.^{23–25}

However, liposomal nanoparticles lack selectivity for cancer cells.²⁶ To overcome this drawback, many researchers have used active targeting strategies by applying targeting ligands such as targeting molecules, antibodies, and peptides to the scaffolds.^{27–31} Active targeting strategies not only enhance drug accumulation in cancer cells, but also diminish toxicity by reducing drug delivery to non-specific tissues.^{15,32–34} However, active targeting strategies for nanoparticles have not always been successful.^{23,35–37} For example, targeted liposomal nanoparticles may fail in their purpose because of differences in tumor model types and PEG coatings, linkers for conjugate targeting ligands, and differences in the properties of targeting ligands.^{38,39}

PEG on PEGylated liposomes performs two roles: (i) it prolongs circulation times by coating the particles, and (ii) it connects a targeting ligand with the liposome. PEG is an ideal molecule to improve the bioavailability of liposomal nanoparticles, although several researchers use PEG with 2000 Da molecular weight (PEG_{2k}) as a linker for traditional reasons rather than scientific considerations.^{40,41} In certain delivery systems, the use of a longer linker, such as PEG with 5000 Da molecular weight (PEG_{5k}), is more appropriate because longer linkers might provide a targeting ligand that is not under the influence of the PEG coating.^{37,41,42} However, several studies have reported that a short linker may afford a more favorable receptor–ligand interaction by limiting the conformational freedom of the ligand.³⁹ Therefore, it is necessary to design an appropriate PEG-linker with a suitable length as a PEG coating for targeted liposome delivery.

Various cancer-cell-specific receptors have been examined for tumor-targeted drug delivery.⁴³ One such receptor is the folate receptor (FR), widely used as a tumor marker. It is expressed only minimally in normal tissues but abundantly in various human tumors such as ovarian cancer cells (IGROV-1, SKOV-3), lung cancer cells (H1299), breast cancer cells (MDA-MB-231, MCF-7), colorectal cancer cells (HCT-116, HT-29), and cervical cancer cells (HeLa, KB, KB-V1).^{44–48} In FR-mediated delivery, folic acid exhibits a high affinity to receptor binding and causes endocytosis, even though it binds covalently to



Scheme 1 Structure of folate-conjugated liposomes (FLs) with different PEG-linker chain lengths and schematic of the behavior of FLs in vivo.

nanoparticles.^{49,50} Liposomes linked with folates via PEG spacers have been utilized to deliver chemotherapeutic drugs and oligonucleotides to tumor cells overexpressing FR, such as KB cells.^{51,52} FR-mediated delivery enhances the cytotoxicity and cellular uptake against FR-expressing tumor cells, which vary depending on the linker length and the presence or absence of PEG coating.^{42,53–55} However, FR-mediated delivery has a few limitations. (i) PEGs of only up to 5K (PEG_{5k}) have been investigated as linkers so far. (ii) Very few in vivo experiments have been conducted. (iii) Finally, no studies have yet been conducted on the biodistribution of linkers based on their length.^{23,42,54,56}

In this study, we develop FR-targeted liposomes with PEG-linkers of various lengths (PEG 2000, PEG 5000, and PEG 10000, denoted as PEG_{2K}, PEG_{5K}, and PEG_{10K}, respectively). Doxorubicin hydrochloride (Dox), a model anticancer drug, was encapsulated in liposomes and assessed for therapeutic efficacy. Physicochemical properties such as particle size, zeta potential, and morphology of liposomal formulations were characterized. Furthermore, the targeting capability of folate-conjugated liposomes (FL) were assessed in vitro and in vivo using human cervical cancer KB cells that overexpress folate receptors on their surface. The overall study is outlined in [Scheme 1](#).

Materials and Methods

Materials

1,2-Distearoyl-sn-glycero-3-phosphoethanolamine-N-[methoxy(polyethylene glycol)-2000] (DSPE-PEG_{2k}), L- α -phosphatidylcholine, hydrogenated (Soy) (HSPC), and cholesterol were obtained from Avanti Polar Lipids Inc. (Alabaster, AL, USA). Folate-conjugated DSPE-PEG (DSPE-PEG_{2k}-Folate) and DSPE-PEG_{2k}-FITC were obtained from Nanocs (New York, USA). Chlorin e6 (Ce6) was purchased from Frontier Scientific (Logan, UT, USA). Dox was purchased from Boryung Co. (Seoul, Korea). KB human nasopharyngeal cancer cells (KB cells) were purchased from the Korean Cell Line Bank (Seoul, South Korea).

Fetal bovine serum (FBS), Dulbecco's phosphate-buffered saline (DPBS), folate-free RPMI 1640 medium, trypsin-EDTA, and penicillin–streptomycin were purchased from Welgene (Gyeongsan-si, Gyeongsangbuk-do, South Korea). The Cell Counting Kit-8 (CCK-8) was obtained from Dojindo Molecular Technologies (Tokyo, Japan). All other chemicals were of analytical grade.

Preparation of Dox-Loaded Folate-Conjugated Liposomes

Liposomes were prepared by a thin-film hydration method, as previously reported.^{17,57} Briefly, HSPC, cholesterol and DSPE-PEG_{2k} were dissolved in chloroform at concentrations of 20 or 10 mg/mL, respectively. To prepare non-targeting liposomes (NTLs) without folate conjugation, a mixture of HSPC (1 mg), cholesterol (0.36 mg), and DSPE-PEG_{2k} (0.32 mg) (55:40:5 molar ratio) was added to chloroform and a thin film was obtained by removing the solvent and drying the remaining mixture in vacuo. To optimize the proportions of the PEG-linker to PEG coating, the ratio of DSPE-PEG_{2k}-Folate was varied from 20% to 80% of the total DSPE-PEG. After fixing the ratio, a mixture of DSPE-PEG_n-Folate (n = 2k, 5k, and 10k for FL-2K, FL-5K, and FL-10K, respectively) and DSPE-PEG_{2k} (molar ratio of 1:4) was used, instead of DSPE-PEG_{2k}, and the FLs were prepared using the same procedure as that used for preparing NTL. The lipid films suspended in deionized water were sonicated for 30 min and extruded as previously reported.⁵⁸ The composition ratios of the prepared liposomes are shown in (Figure 1a) and Table S1.

Dox-loaded NTL (Dox/NTL) or FL (Dox/FL) was obtained by the remote loading method using the Sephadex G-25 column (GE Healthcare, Buckinghamshire, UK).^{51,59} Briefly, the prepared thin films were suspended in an ammonium sulfate solution (300 mM), and the liposomal solution was sonicated and extruded. The liposomal solution was passed through a Sephadex G-25 column using the HEPES buffer (10 mM, pH 7.4) to remove the free ammonium sulfate solution and to obtain pH gradient condition. The liposomal solution was incubated with the Dox solution for 2 h at 60 °C. The liposomes were then passed through a Sephadex G-25 column to separate the free Dox from that entrapped in the liposome.

Characterization of the Prepared Liposomes

To characterize the prepared liposomes, the effective hydrodynamic diameters (D_{eff}), particle size distribution, and zeta potential of the prepared liposomes were determined by photon correlation spectroscopy using Zetasizer Nano-ZS (Malvern Instruments, Worcestershire, UK) equipped with a multi-angle sizing option (BI-MAS).^{16,57} Before performing the measurements, all sample solutions were incubated at 25 °C for 30 min. Each sample was measured thrice to determine their respective D_{eff} , polydispersity index (PDI), and zeta potential values.

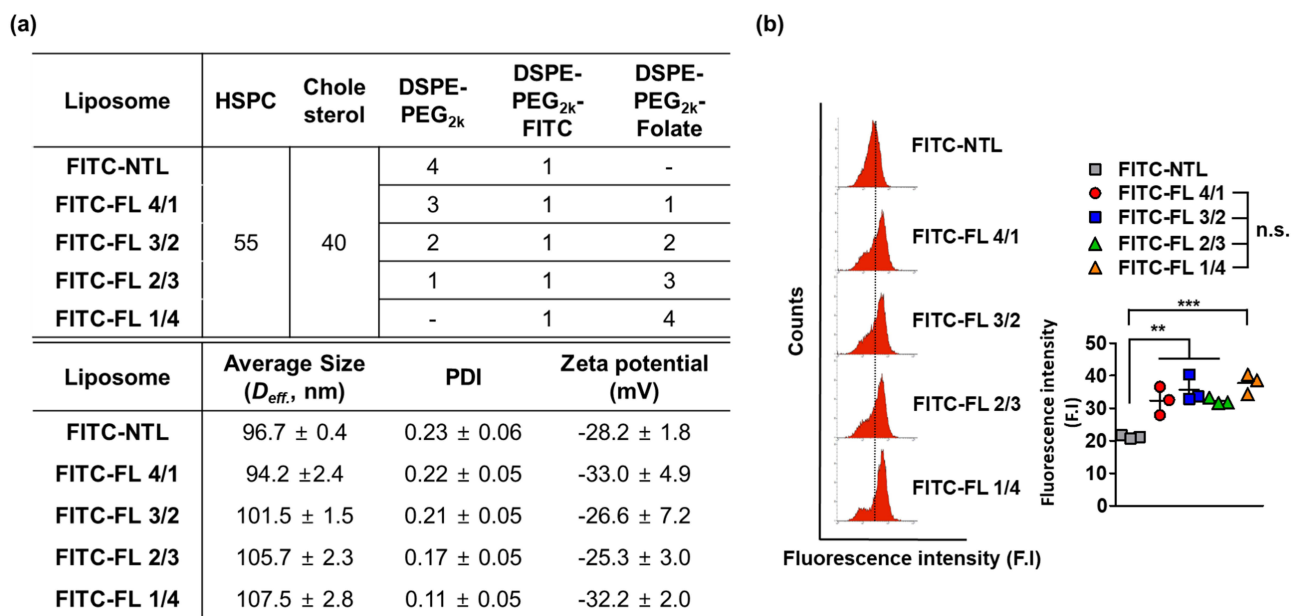


Figure 1 Preparation and characterization of FITC-labeled folate-conjugated liposomes (FITC-FLs). (a) Composition of liposomes (molar ratio %), particle size, polydispersity index (PDI), and zeta potential of liposomes. (b) Flow cytometric analysis of cellular uptake 5 h after sample treatment.

Notes: **($p < 0.01$), and ***($p < 0.001$).

Abbreviation: n.s., not significant.

Morphologies of the prepared liposomes were investigated using FE-SEM (Carl Zeiss Meditec AG, Jena, Germany). The formulation samples were dropped on a glass slide and dried in vacuo. The sample surfaces were coated with platinum using ion sputtering and then their microphotographs were obtained.

Next, the drug-incorporating efficiency and content were evaluated. The liposomes were dissolved in 1% Triton X-100 aqueous solution to destroy liposomal vesicles and were then analyzed using a UV-1200 spectrophotometer (Labentech, Incheon, Korea) at 481 nm. The Dox-loading efficiency and content were determined using the following equations:

$$\text{Drug – loading efficiency (wt\%)} = \frac{\text{weight of drug in liposomes (mg)}}{\text{weight of initially adding drug to formulation (mg)}} \times 100$$

$$\text{Drug – loading efficiency (wt\%)} = \frac{\text{weight of drug in liposomes (mg)}}{\text{weight of initially adding drug to formulation (mg)}} \times 100$$

Cellular Uptake and in vitro Cytotoxicity Assay

Human cervical cancer KB cells were cultured in folate-free RPMI supplemented with 10% FBS and 1% penicillin–streptomycin. The cellular uptake of the liposomes was determined by confocal microscopy and flow cytometry using KB cells in folate-free media. For confocal imaging, the KB cells (40×10^4 cells/well) were seeded in each confocal dish. After 24 h of incubation, they were treated with Free Dox, Dox/NTL, Dox/FL-2K, Dox/FL-5K, or Dox/FL-10K. The samples were then prepared for assessment, as mentioned previously.^{42,54,60} Briefly, after 5 h of sample treatment, the cells were washed thrice with cold PBS and incubated with the Vectashield mounting medium containing 4',6-diamidino-2-phenylindole (Vector Laboratories, Burlingame, CA, USA) for 15 min. The treated cells were analyzed under a confocal microscope (LSM 510 Meta, Carl Zeiss AG, Jena, Germany). For flow cytometry analysis, the KB cells (20×10^4 cells/well) were seeded in 12-well plates. The next day, the cells were treated with FITC-NTL or FITC-FLs for 5 h. The cells were washed thrice with cold PBS and harvested by adding the 200 μ L of trypsin in each well. The FITC fluorescence intensity was analyzed with a FACSCalibur flow cytometer and Cell Quest Pro software (BD Biosciences, San Diego, CA, USA).⁶¹ For the folate-competition study, the KB cells cultured in 1mM folate containing RPMI medium were seeded in 12-well plates (20×10^4 cells/well), and the cells were treated with Dox-loaded liposomal formulations for 5 h. The cells were washed thrice with cold PBS and the Dox fluorescence intensity was analyzed with a FACSCalibur flow cytometer and Cell Quest Pro software (BD Biosciences, San Diego, CA, USA). For cytotoxicity of the formulations, 10^4 of KB cells in 96-well plates were treated with Free Dox, Dox/NTL, Dox/FL-2K, Dox/FL-5K, or Dox/FL-10K (0.001–10 μ g/mL) for 48 h. The cell viability was measured using CCK-8.

Bovine Serum Albumin (BSA) Binding Analysis

Any change in the intrinsic fluorescence of tryptophan residues within the BSA caused by Free Dox, Dox/NTL, Dox/FL-2K, Dox/FL-5K, or Dox/FL-10K was evaluated. Briefly, samples containing various concentrations of Dox were added to 1 mg/mL of BSA in pH 7.4 PBS solution and mixed for 30 min. Then, using a Scinco FS-2 fluorescence spectrometer, the emission spectra were recorded from 300 to 500 nm after excitation at 280 nm. The excitation/emission slits were set at 5 nm.^{62,63}

Animal Care

All animal care and experiments were performed under the protocol approved by the Institutional Animal Care and Use Committee of Chung-Ang University (Seoul, Republic of Korea) and the National Institute of Health guidelines (“Guide for the care and use of laboratory animals” and “Animal Protection Law in Republic of Korea”). The experimental protocol was approved by the Institutional Animal Care and Use Committee of the Chung-Ang University of Korea (approval number: 2020–00071).

In vivo Tumor Inhibition

To establish tumor xenografts, KB cell suspensions at a density of 5×10^6 cells were injected subcutaneously into the right flank of 4-week-old female nude mice (BALB/c, nu/nu mice; Nara Biotech, Seoul, South Korea). The tumor volume was analyzed using the following equation.

$$\text{Tumor volume} = \text{length} \times \frac{(\text{width})^2}{2}$$

All in vivo studies were initiated when the tumor volume reached approximately 50–100 mm³.

The KB tumor-bearing mice were randomly divided into six groups. On days 1 and 4, the mice were intravenously injected via tail vein with various samples, including saline (as a control group), Free Dox, Dox/NTL, Dox/FL-2K, Dox/FL-5K, and Dox/FL-10K, with each sample containing a dose of 4 mg/kg of Dox. Changes in the tumor size and body weight were checked for 24 days.

In vivo Fluorescence Imaging

To study biodistribution of the prepared liposomes, Ce6 was used as a dye to obtain fluorescence images in real time. To prepare the Ce6-loaded NTL or FLs (Ce6/NTL, Ce6/FL-2K, Ce6/FL-5K, or Ce6/FL-10K), Ce6 was added into the lipid mixture and the subsequent process was performed as described before. Ce6/NTL, Ce6/FL-2K, Ce6/FL-5K, or Ce6/FL-10K was injected into the tail veins of mice bearing KB tumors at the same amounts of Ce6. The biodistribution of liposomes as a function of time after injection was monitored using a Fluorescence In Vivo Imaging System (FOBI system, Neo Science, Suwon, South Korea). At 48 h post-injection, the nude mice were sacrificed, and the tumor and various organs were collected to analyze ex vivo fluorescence levels.

Statistical Analysis

GraphPad 5.0 was used for the statistical analysis. Numerical results are expressed as mean \pm standard deviation in figures and tables.⁶⁴ For comparison within two groups, an unpaired two-tailed *t*-test was conducted.⁶⁵ For comparison among multiple groups, one-way analysis of variance (one-way ANOVA) with Turkey's test or two-way ANOVA by Bonferroni post-tests were employed for statistical analysis (Tables S2–S5).⁶⁶ **P* < 0.05, ***P* < 0.01, ****P* < 0.001.

Results and Discussion

Preparation and Characterization of Folate-Conjugated Liposomes

PEGylated liposomal nanoparticles are widely utilized in drug-delivery systems because of their advantages such as increased stability and long circulation time.^{20,67} The liposomes prepared in this study comprised HSPC, DSPE-PEG_{2k}, and cholesterol (55:5:40 molar ratio). This composition is similar to that of liposome Doxil, approved by the Food and Drug Administration.^{19,68}

Folate is a ligand with high affinity for FR (*K_d* = 0.1 nM). It has 38-kDa glycosyl-phosphatidylinositol membrane-anchored glycoproteins, which are overexpressed in KB cells.⁴⁴ On binding to its receptor, the glycoprotein is internalized through receptor-mediated endocytosis.⁴⁹ The folate-targeting strategy affords a higher cellular uptake than that achieved by the non-targeting strategy in vitro. However, this strategy is affected by various factors, including the PEGylation of particles, length of the PEG-linker conjugated with the folate, and ligand density per drug carrier.^{69–71}

Here, we evaluated how the cellular uptake efficiency of liposomes changes when folate is conjugated to the liposome surface. The ratio of DSPE-PEG_{2k}-Folate varied from 20% to 80% when the total DSPE-PEG and DSPE-PEG_{2k}-FITC was fixed at 20%. Next, the particle size, PDI, and zeta potential of the prepared liposomes were evaluated. All the formulations had ~100-nm particles with a narrow size distribution. In addition, the zeta potential of the particles was around –30 mV; however, no significant differences were observed between the formulations (Figure 1a). When the KB cells were treated with formulations in vitro, the cellular uptake efficiency of the FL dramatically increased compared to that of the NTL. This phenomenon is caused by the increased interaction between the FR overexpressed on the KB cell surface and the liposomes decorated with the folate ligand. However, the cellular uptake efficiency for each formulation did not change significantly when the folate ratio was $\geq 20\%$ (Figure 1b).

Characterization of Folate-Conjugated Liposomes at Different PEG-Linker Lengths

Decorating 20% of the total DSPE-PEG with folate was sufficient to target the FR overexpressed on the KB cell surface. Therefore, after fixing DSPE-PEG_{2k}-Folate to 20%, the length of the PEG-linker was varied to check various physico-chemical properties before and after drug encapsulation. First, the morphology and size distribution were investigated after encapsulation of the model drug, Dox, into each liposomal formulation. Regardless of the PEG length, all formulations showed spherical morphology with narrow size distribution (Figure 2a). Next, the particle size, PDI, and zeta potential values of each formulation were investigated. When Dox was encapsulated in the liposome system, the particle size slightly increased. No dramatic change in the particle size occurred, although a change in the length of the PEG-linker was observed. As the length of the PEG-linker increased, the zeta potential of the particles decreased. The zeta potential of the NTLs was approximately -25 mV. The negative value of zeta potentials could be due to the occurrence of DSPE-PEG_{2k}, a negatively charged lipid, in the formulation.^{72,73} As the length of the PEG-linker increased, the negative charge on the surface decreased and became -20 mV. This might be related to the shift in the hydrodynamic phase of shear away from the liposome surface. The long PEG may also decrease the Brownian motion of liposomes (Figure 2b).^{74,75} The zeta potential value of liposomal formulation could be changed due to the effect of the PEG-linker length. However, this may not be a sufficient explanation because the PEG-linker accounts for only 20% of the total PEG. Therefore, additional characterization data of PEG-Liposomal formulations with various PEG molecular weights were added. When the non-targeted liposomal formulations (NTL) were prepared with 2K, 5K, and 10K PEG (DSPE-PEG_{2K}, _{5K}, or _{10K}), there were no big changes in particle size (Figure S1a). However, the zeta potential value of 5K and 10K PEG based formulations were more dramatically decreased compared to that of the FL-5K and FL-10K (Figure S1b). These data strongly support that PEG neutralizes surface charge by sterically protecting membranes with increasing length. The prepared liposomes showed good stability in aqueous solutions without any change in their particle size and precipitation for 28 days (Figure 2c).

Cellular Uptake and in vitro Cytotoxicity

To investigate the influence of the length of PEG-linkers for targeting KB cells, the cellular uptake of liposomes with PEG-linkers of different molecular weights was evaluated. As shown in the confocal fluorescence imaging (Figure 3a), the Dox-loaded liposomal formulations were translocated into cells (red). The red fluorescence was more vivid in the cells treated with Dox/FLs than that of the Dox/NTL-treated groups. The difference in cellular uptake between FITC-labeled liposome-treated groups was quantitatively analyzed using flow cytometry (Figure 3b). Clearly, the level of cellular uptake of FLs increased by >1.8 times compared to that achieved with NTL; no significant differences among the FLs based on the length of PEG-linkers were observed. However, the cellular uptake may vary kinetically, depending on the incubation time of the sample. Note that no significant change was observed under the 5-h incubation condition. A folate-competition experiment conducted using folate-pretreated media did not show any difference in the tested formulations (Figure S2). This result indicates that free folate hamper the enhanced cellular uptake of FL^{42,54} and that the intracellular uptake occurred by receptor-mediated endocytosis.⁷⁶

The cytotoxicity of NTL and FLs against KB cells was assessed based on a cell-viability test conducted by a CCK assay under a series of equivalent concentrations of Dox for 48 h. The IC₅₀ values ($\mu\text{g/mL}$) of the Free Dox, Dox/NTL and FLs (2K/5K/10K) were 0.0896, 0.1214, 0.1197, 0.1077, and 0.1125, respectively. However, no significant differences between the liposomal formulations were observed (Figure 3c). These data suggest that folate decoration on the liposome surfaces could enhance the cellular uptake efficiency; however, this difference could decrease over time, leading to a similar anticancer activity of the formulated drug in vitro.

We also investigated the level of quenching of the fluorescence of tryptophan residues within the BSA, which could be used to evaluate the drug-protein binding affinity (Figure 3d). Compared to Free Dox, Dox in liposomal formulations significantly reduced the quenching level of tryptophan, which demonstrates that encapsulation of drugs into liposomes reduces albumin binding. However, no difference was observed when liposomal formulations at different PEG-linkers were compared.

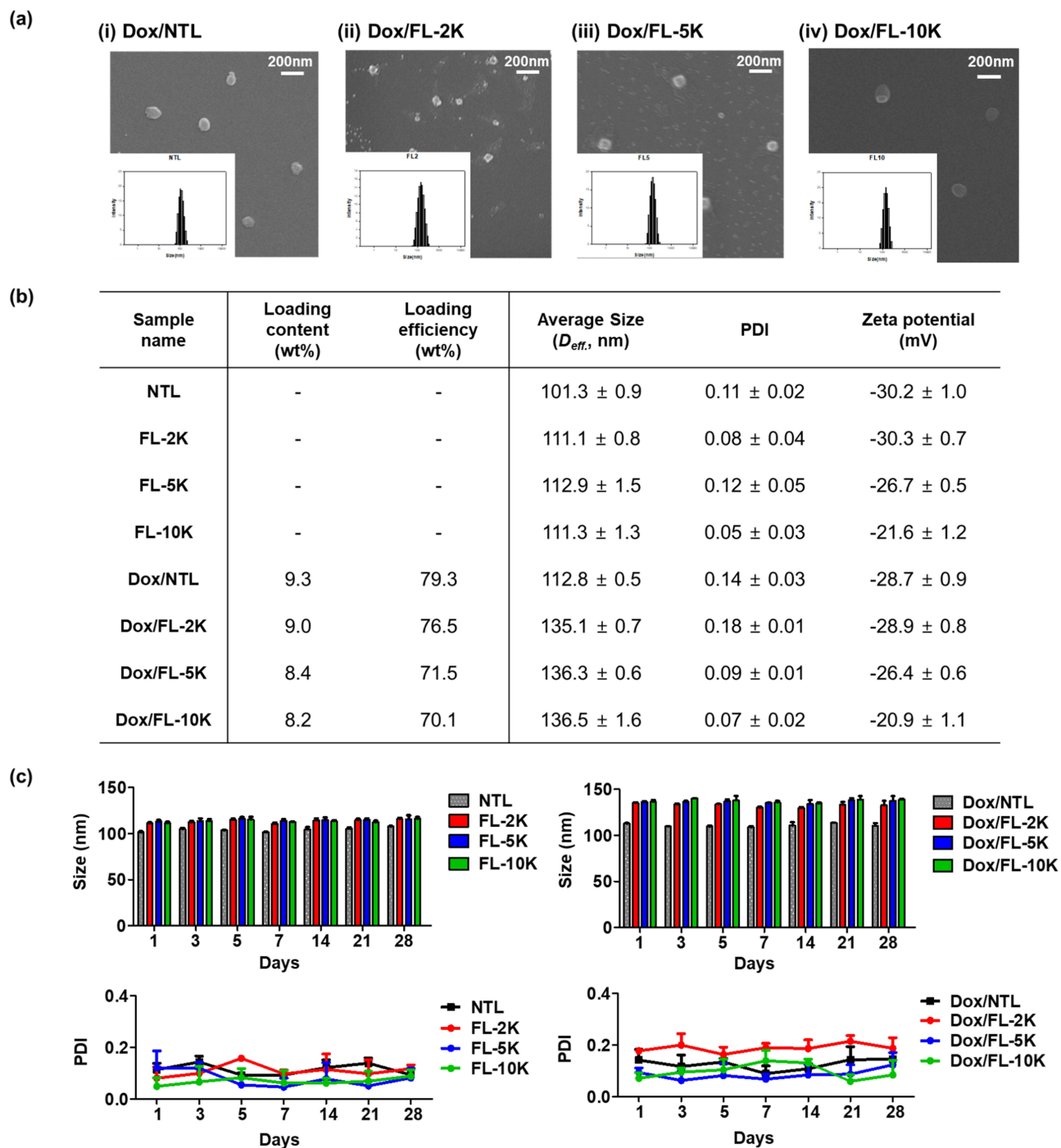


Figure 2 Physicochemical characterization of folate-conjugated liposomes (FL). (a) Morphology and size distribution of Dox-loaded folate-conjugated liposomes (Dox/FL) at various PEG-linker lengths. (b) Loading content, loading efficiency, particle size, polydispersity index (PDI), and zeta potential of prepared liposomes. (c) Stability of FLs or Dox/FLs at various PEG-linker lengths.

Effect of PEG-Linker Length on Distribution of Liposomal Formulation at Tumor Site

To compare the tumor-targeting ability of FLs *in vivo* depending on the length of PEG-linkers, time-dependent biodistribution was evaluated in live and subcutaneous KB cell xenograft mouse model with Ce6-loaded liposomes (Ce6/NTL, Ce6/FL-2K, Ce6/FL-5K, and Ce6/FL-10K). The formulations were injected into the tail vein of the tumor-bearing nude mice. All groups showed a gradual increase in fluorescence intensity at the tumor site (Figure 4a). This result could be due to liposome coating via DSPE-PEG. The PEG-coated liposomes could extend the blood circulation time of the particles by avoiding the immune system

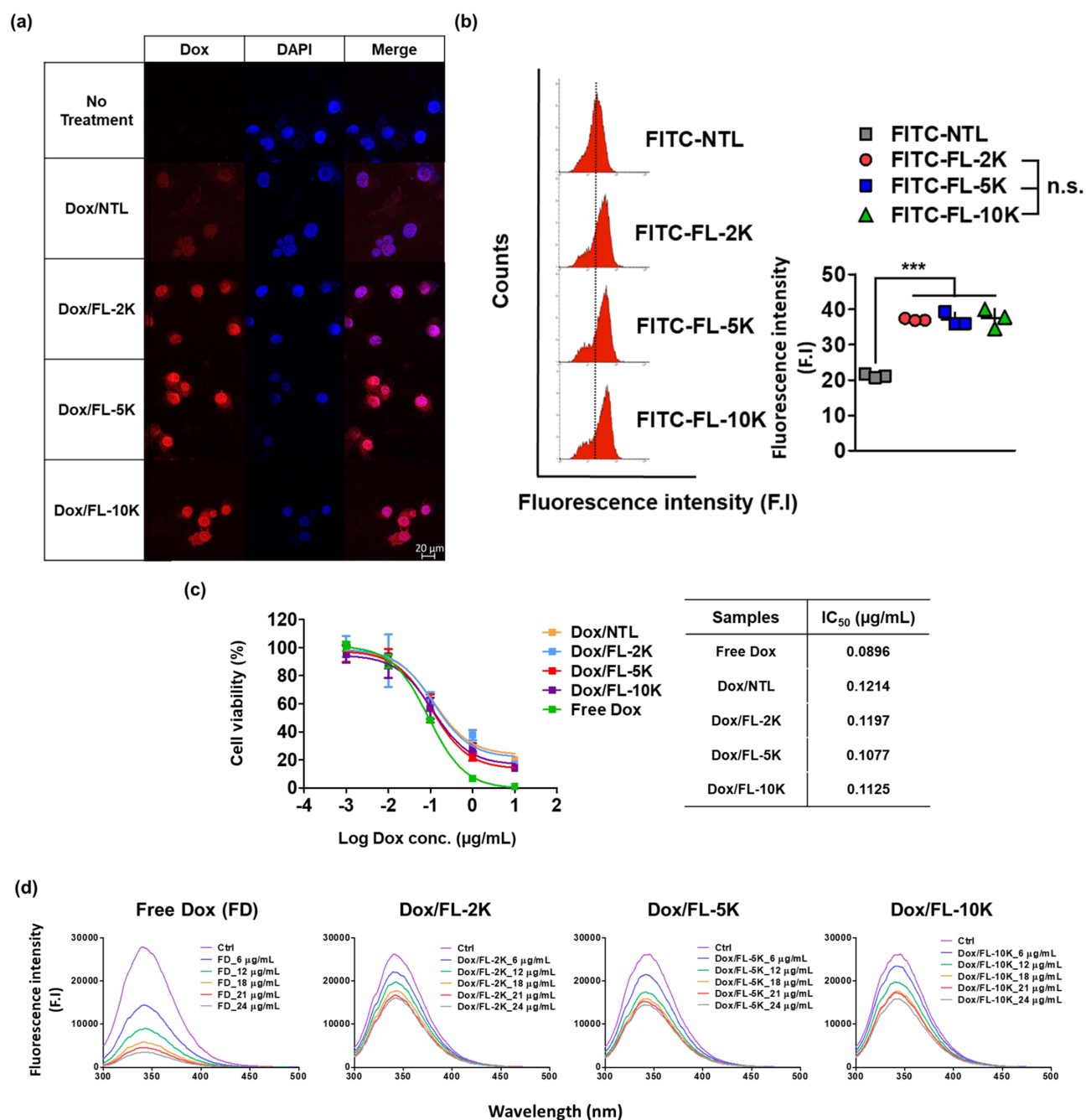


Figure 3 In vitro evaluation of FLs. (a) Confocal assay of cellular uptake of Dox/FLs and (b) flow cytometric analysis of cellular uptake of FITC-FLs 5 h after sample treatment. (c) Cytotoxicity of Dox in KB cell line. (d) Tryptophan fluorescence quenching assay by adding either Free Dox, Dox/FL-2K, Dox/FL-5K, or Dox/FL-10K at a given concentration of Dox.

Note: ***($p < 0.001$).

Abbreviation: n.s., not significant.

and accumulating at the tumor site owing to the EPR effect.^{5,20} Here, the fluorescence intensity of the Ce6/FL-10K-treated group was significantly higher than that of the group treated by other formulations. To quantitatively confirm the fluorescence intensity, the main organs and the tumor were excised from the sacrificed mice 48 h after injection (Figure 4b and c). All the FLs showed better accumulation at the tumor site than that of NTL. In addition, the Ce6/FL-10K group showed significantly enhanced fluorescence intensity at the tumor site, clearly demonstrating the effect of PEG-linker length on tumor targeting in vivo.

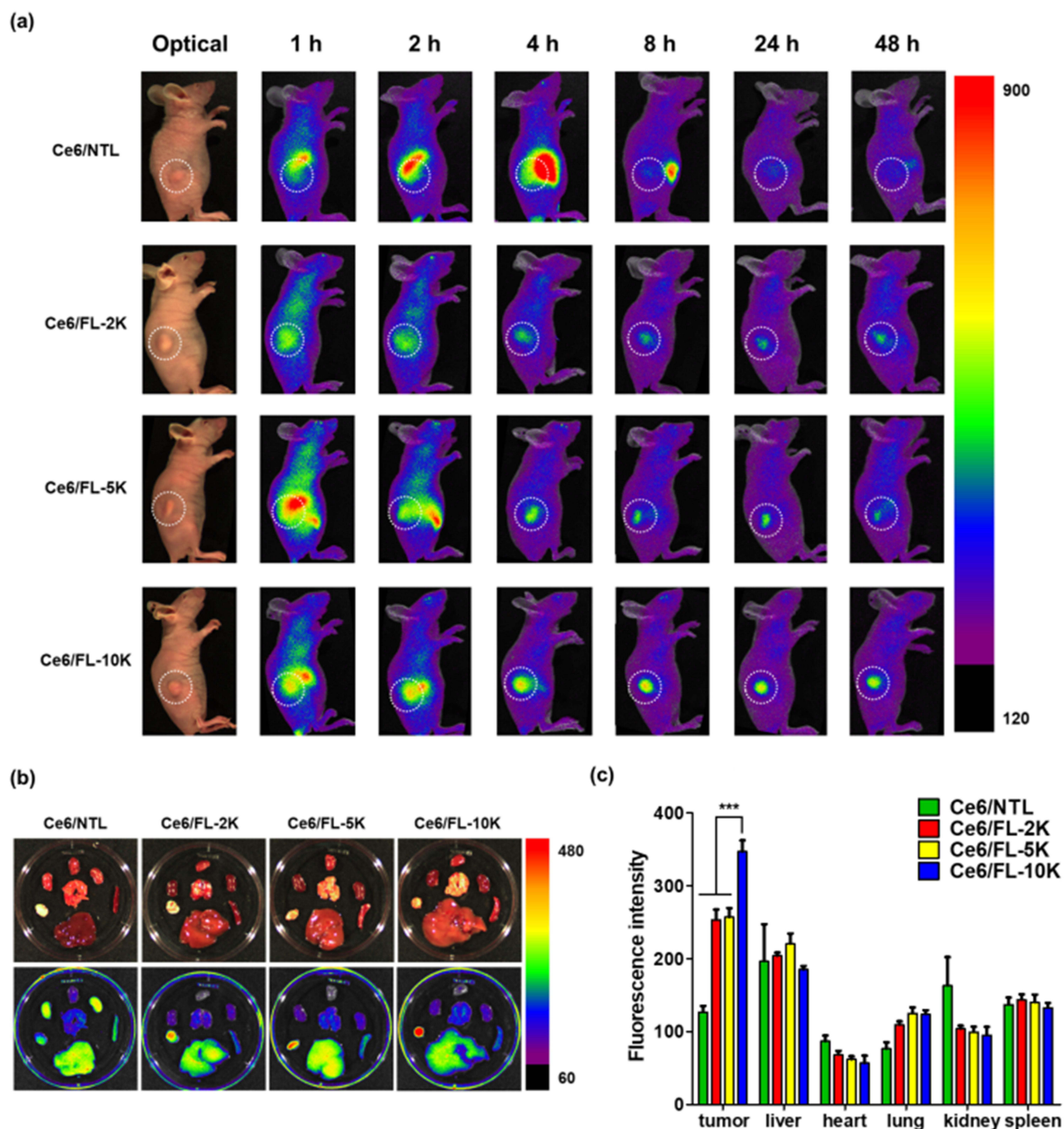


Figure 4 Distribution of Ce6-loaded PEG-Lipo formulations (Ce6/NTL or Ce6/FLs) in KB tumor-bearing mice. (a) Non-invasive whole-body imaging at given time points. (b) Fluorescence image of harvested organs (tumor, liver, heart, lung, kidney, and spleen) 48 h after sample injection. (c) Quantitative fluorescence intensities of tumors and main organs.

Note: ***($p < 0.001$).

In vivo Tumor Inhibition

We further explored the antitumor activity of Dox in the KB tumor-bearing mouse model by intravenously administrating Free Dox or Dox-loaded liposomes at 4 mg/kg (equivalent Dox concentration) twice a week. All liposomal formulations showed a significant antitumor activity and inhibited the tumor growth (Figure 5a). In addition, when the folate was conjugated to the surface of the liposome, the tumor growth dramatically delayed compared to that observed with the

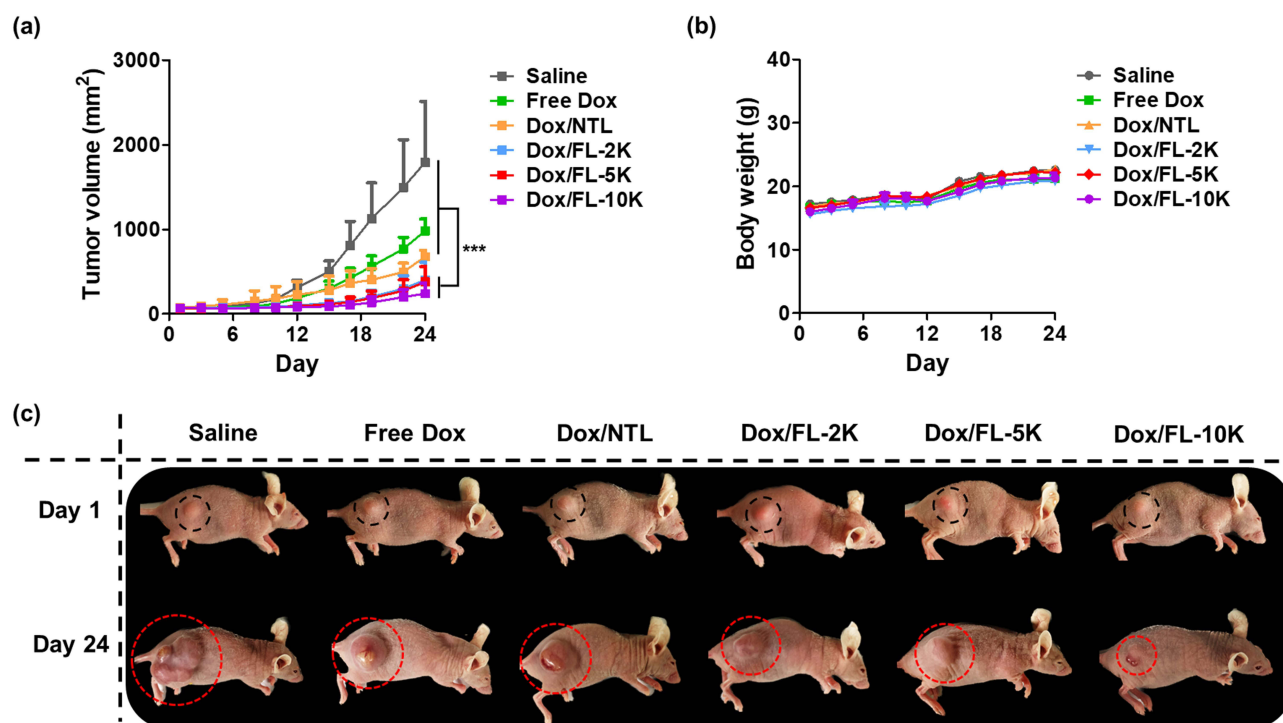


Figure 5 In vivo characterization. (a) In vivo antitumor activity, and (b) body weight changes in KB tumor-bearing nude mice after intravenous administration of saline, Free Dox, and Dox-loaded liposomes. (c) Optical images of tumor-bearing mice at days 1 and 24. **Note:** ***($p < 0.001$).

NTL-treated group. However, no dramatic changes in body weight were observed in all groups, which suggested that the treatments did not induce any systemic toxicity (Figure 5b). Optical images of tumor tissue are presented in (Figure 5c).

The above results suggest that the FR targeting strategy via liposomal formulation is effective even under in vivo conditions. However, unlike the previous results on particle distribution, the length of the folate-conjugated PEG-linker did not have a great effect on the therapeutic efficacy of the encapsulated drug. Clearly, the growth rate of the tumor was slower in the Dox/FL-10K-treated group than that in the Dox/FL-5K- or Dox/FL-2K-treated groups, although no statistical difference was observed between the groups. This occurred probably because the effect of the PEG-linker length is somewhat reduced because of the continuous release of the drug from the formulation after administration in vivo. Overall, folate conjugation showed a clear targeting effect under in vivo conditions, and as the length of the PEG-linker increased, the PEGylation effect became stronger, and the targeting ability further increased.

Discussion

We evaluated the effect of the PEG-linker length of FL on the treatment of FR-overexpressing solid cancers. Here, to sufficiently expose the targeting moiety in the shell part of the liposomal formulation, PEG 2K was used as a component of the liposomal vehicle. Then, the targeting comparison study was performed using a molecular weight of 2K or higher for the PEG linker length. FLs were formulated by preparing three types of PEG-linkers (FL-2K, FL-5K, and FL-10K) and fixing the length of the coated PEG to 2K. Regardless of the length of the PEG-linker, all liposomes were of 110–140 nm with a spherical shape. However, the zeta potential of the formulations increased when the linker length increased. Because of the lipid present on the particle membrane, the formulations have a negatively charged surface. However, as the length of PEG increases, it sterically protects the membrane, thereby neutralizing the surface charge.

In our previous study, we had reported that the zeta potential further increased to -10 mV when the entire liposome was coated with 10K PEG without any decoration. In contrast, when the liposome surfaces were coated with 2K PEG (DSPE-PEG_{2k}), the zeta potential was approximately -30 mV. This result is similar to our current research trend and proves that the surface becomes more neutral as the PEG layer is increased.

We compared the targeting ability of folate ligand conjugated liposomal formulation against two cell lines (KB cell and SKOV-3 cell) that is known to have overexpressed folate receptor on the surface. As shown in [Figure S3](#), we confirmed that the folate receptor targeting ability of FITC-FL (FITC and Folate ligand conjugated liposomal formulation) was higher in the KB cell lines than that of SKOV-3 cell lines. Thus, we used KB cells as a model cell line in this study.

We demonstrated that the rates of intracellular uptake of nanoparticles in KB cells increased when the surface is decorated with folate. However, when evaluating the cell viability, no significant difference was observed between NTL and FL. As the cells and the liposomal formulations continuously interact with each other and the drug is also continuously released during the 48-h incubation under the *in vitro* condition, the PEG-linker difference could be ignored.

When the effect of the PEG-linker length on the cellular uptake efficiency is compared, no significant difference was observed under 5-h incubation. Hence, the length of the PEG-linker is not a very important *in vitro* condition. However, it should be considered that the binding affinity between the PEG-linker lengths of liposomes and the FR-overexpressed cell membrane could be kinetically changed. Interestingly, the level of tumor accumulation of particles significantly changed based on the length of the PEG-linker under *in vivo* condition. The longer the length of the PEG-linker is, the stronger the targeting ability is. However, this should be interpreted as a complex phenomenon that appears as the PEGylation effect becomes stronger owing to the increase in the length of the PEG-linker.

In our previous study, we did not observe any difference in terms of tumor accumulation and antitumor activity between the liposomes coated with 5K PEG (DSPE-PEG_{5k}) and 10K PEG (DSPE-PEG_{10k}). In contrast, in the present study, significant changes were observed, depending on the lengths of 5K and 10K PEG-linkers, which can be seen as the PEG-linker playing a complex role along with PEGylation *in vivo*.

When the antitumor activity is compared, the difference between Dox/FL-10K and other formulations was not significant under the two-way ANOVA analysis condition. However, when looking at the tumor size as an absolute value, the average tumor size in the Dox/FL-10K-treated group reduced by >40% compared to that in other Dox/FL-treated groups. This difference may further increase, depending on the number of drugs administered, the frequency of the administration, and the dosing amount. In general, a drug is continuously and rapidly released after its nanoformulation is administered *in vivo*. Because of the different drug-release patterns, there may a slight reduction in the antitumor activity of the drug, depending on the length of the PEG-linker.

Similar studies to this research have been conducted by various groups. For example, Fazhan Wang et al, conducted research on delivering mRNA using mannose-conjugated liposomes.⁷⁷ They varied the length of PEG linker to 100, 1000, and 2000 to explore its impact on mRNA delivery. Hang Xing et al also conducted research on targeted drug delivery using liposomes conjugated with aptamers with different linker length.⁷⁸ While both studies emphasized the variation in targeting effect by adjusting the linker length, they are limited to *in vitro* experiments. Phei Er Saw et al conducted research on targeted drug delivery using liposomes conjugated with peptides that target fibronectin.³⁸ This study also varied the length of the PEG linker to investigate its importance in *in vitro* and *in vivo* experiments. However, their research screened PEG lengths from 550 Da to 2 kDa. In contrast, our study varied PEG lengths from 2 kDa to 10 kDa and found that the effect was most enhanced when the PEG linker was lengthened up to 10 kDa, which had not been previously confirmed. This emphasizes the novelty of our study.

In our study, the length of the PEG-linker demonstrated a more significant effect *in vivo* than *in vitro*. This is because under *in vitro* conditions, nanoparticles constantly interact with cell membranes, resulting in a kinetic variation in cellular uptake efficiency. However, *in vivo*, nanoparticles operate in a more dynamic and systemic manner, highlighting the importance of *in vivo* evaluation and revealing a clearer demonstration of the effect of the PEG-linker length.

Fluorescence dyes can be used to track the distribution of nanoparticles *in vivo*. However, it is important to note that fluorescence imaging has limitations in terms of depth penetration and tissue autofluorescence, which can affect the sensitivity and specificity of detection. The suitability of a fluorescence dye for *in vivo* imaging depends on several factors, including its excitation and emission range. Doxorubicin's fluorescence properties are not typically strong enough for *in vivo* tracking of nanoparticles. The excitation and emission ranges for optimal imaging are typically in the visible or near-infrared range, where tissue autofluorescence is relatively low. However, doxorubicin's excitation and emission wavelengths of 470 nm and 590 nm, respectively, do not match these ranges. Therefore, other fluorescent dyes such as chlorin e6, which have higher excitation and emission ranges, are typically preferred for *in vivo* tracking of nanoparticles.

Positioning of the targeting moiety can have a significant impact on targeting efficiency, depending on whether it is located on the inside or outside of the liposome. However, in the sample preparation method used in our study, it is unclear whether the folate ligand is distributed more on the inside or outside, and it can generally be assumed to be randomly and evenly distributed. To address this issue, some studies prepare drug-loaded liposomes first and then conjugate the targeting moiety in the final stage.^{79–82} However, this approach may not be preferred from a translational perspective due to problems such as drug linkage during conjugation and removal step of unconjugated ligand.

In future research, it will be necessary to compare the targeting efficiency of liposomal formulations by conjugating the targeting ligand directly onto pre-made nanoparticles. This will ensure that all ligands are exposed to the surface, thus enabling a more accurate assessment of the impact of the ligand on targeting efficiency. Additionally, the optimization of the ligand conjugation process is also essential to address various issues such as stability, drug leakage, purification, and any other potential problems that may arise.

Conclusion

In conclusion, this study aimed to evaluate the impact of PEG-linker length on the distribution and pharmacological efficacy of folate-conjugated liposomes encapsulating Dox in vitro and in vivo. The results indicated that the cellular uptake efficiency in folate receptor-overexpressing cells increased significantly with folate-conjugated liposomes, and the length of PEG-linkers was crucial to the tumor-targeting ability and pharmacological effects of encapsulated drugs in vivo. Specifically, the level of tumor accumulation of particles significantly increased as the length of the PEG-linker was increased, resulting in a more than 40% reduction in tumor size in the Dox/FL-10K-treated group compared to the Dox/FL-2K- or 5K-treated groups. This study provides valuable insights for the development of ligand-conjugated liposomes for the treatment of specific receptor-overexpressing cancers.

Acknowledgments

This research was supported by the Chung-Ang University Graduate Research Scholarship in 2021 and by the National Research Foundation of Korea (NRF) grant funded by the Korea government (MSIT) (No. 2021R1A2C2008519 and 2022R1A5A6000760).

Disclosure

There are no conflicts of interest to declare.

References

1. Atlihan-Gundogdu E, Ilem-Ozdemir D, Ekinci M, et al. Recent developments in cancer therapy and diagnosis. *J Pharm Investig.* 2020;50:1–13.
2. Tran P, Lee S-E, Kim D-H, Pyo Y-C, Park J-SJ. Recent advances of nanotechnology for the delivery of anticancer drugs for breast cancer treatment. *J Pharm Investig.* 2020;50(3):261–270.
3. Gupta B, Kim JOJ. Recent progress in cancer immunotherapy approaches based on nanoparticle delivery devices. *J Pharm Investig.* 2021;51:1–14.
4. Ha E-S, Kang H-T, Park H, Kim S, Kim M-S. Advanced technology using supercritical fluid for particle production in pharmaceutical continuous manufacturing. *J Pharm Investig.* 2022;2022. doi:10.1007/s40005-022-00601-y
5. Doane TL, Burda C. The unique role of nanoparticles in nanomedicine: imaging, drug delivery and therapy. *Chem Soc Rev.* 2012;41(7):2885–2911. doi:10.1039/C2CS15260F
6. Wagner V, Dullaart A, Bock A-K, Zweck A. The emerging nanomedicine landscape. *Nat Biotechnol.* 2006;24(10):1211–1217. doi:10.1038/nbt1006-1211
7. Kiiro TM, Park SJ. Physical properties of nanoparticles do matter. *J Pharm Investig.* 2021;51(1):35–51.
8. Hoang NH, Lim C, Sim T, Oh KT. Triblock copolymers for nano-sized drug delivery systems. *J Pharm Investig.* 2017;47(1):27–35. doi:10.1007/s40005-016-0291-7
9. Son G-H, Lee B-J, Cho C-W. Mechanisms of drug release from advanced drug formulations such as polymeric-based drug-delivery systems and lipid nanoparticles. *J Pharm Investig.* 2017;47(4):287–296. doi:10.1007/s40005-017-0320-1
10. Uhrich KE, Cannizzaro SM, Langer RS, Shakesheff KM. Polymeric systems for controlled drug release. *Chem Rev.* 1999;99(11):3181–3198. doi:10.1021/cr940351u
11. Cho H-J. Recent progresses in the development of hyaluronic acid-based nanosystems for tumor-targeted drug delivery and cancer imaging. *J Pharm Investig.* 2020;50(2):115–129.
12. Shinn J, Kwon N, Lee SA, Lee Y. Smart pH-responsive nanomedicines for disease therapy. *J Pharm Investig.* 2022;52(4):427–441. doi:10.1007/s40005-022-00573-z
13. Hua S, Wu S. The use of lipid-based nanocarriers for targeted pain therapies. Mini Review. *Front Pharmacol.* 2013;4(143). doi:10.3389/fphar.2013.00143

14. Lim C, Kang JK, Won WR, et al. Co-delivery of D-(KLAKLAK)₂ peptide and chlorin e6 using a liposomal complex for synergistic cancer therapy. *Pharmaceutics*. 2019;11(6):293. doi:10.3390/pharmaceutics11060293
15. Nogueira E, Gomes AC, Preto A, Cavaco-Paulo A. Design of liposomal formulations for cell targeting. *Colloids Surf B Biointerfaces*. 2015;136:514–526. doi:10.1016/j.colsurfb.2015.09.034
16. Patil Y, Amitay Y, Ohana P, Shmeeda H, Gabizon A. Targeting of pegylated liposomal mitomycin-C prodrug to the folate receptor of cancer cells: intracellular activation and enhanced cytotoxicity. *J Control Release*. 2016;225:87–95. doi:10.1016/j.jconrel.2016.01.039
17. Sadzuka Y, Sugiyama I, Tsuruda T, Sonobe T. Characterization and cytotoxicity of mixed polyethyleneglycol modified liposomes containing doxorubicin. *Int J Pharm*. 2006;312(1):83–89. doi:10.1016/j.ijpharm.2005.12.043
18. Hegde MM, Prabhu S, Mutalik S, Chatterjee A, Goda JS, Satish Rao BS. Multifunctional lipidic nanocarriers for effective therapy of glioblastoma: recent advances in stimuli-responsive, receptor and subcellular targeted approaches. *J Pharm Investig*. 2022;52(1):49–74. doi:10.1007/s40005-021-00548-6
19. Gabizon A, Shmeeda H, Barenholz Y. Pharmacokinetics of pegylated liposomal doxorubicin. *Clin Pharmacokinet*. 2003;42(5):419–436. doi:10.2165/00003088-200342050-00002
20. Hamidi M, Azadi A, Rafiei P. Pharmacokinetic Consequences of Pegylation. *Drug Deliv*. 2006;13(6):399–409. doi:10.1080/10717540600814402
21. Muthu MS, Kulkarni SA, Xiong J, Feng -S-S. Vitamin E TPGS coated liposomes enhanced cellular uptake and cytotoxicity of docetaxel in brain cancer cells. *Int J Pharm*. 2011;421(2):332–340. doi:10.1016/j.ijpharm.2011.09.045
22. Singh S. Liposome encapsulation of doxorubicin and celecoxib in combination inhibits progression of human skin cancer cells. *Int J Nanomedicine*. 2018;13:11–13. doi:10.2147/IJN.S124701
23. Noble GT, Stefanick JF, Ashley JD, Kiziltepe T, Bilgicir B. Ligand-targeted liposome design: challenges and fundamental considerations. *Trends Biotechnol*. 2014;32(1):32–45. doi:10.1016/j.tibtech.2013.09.007
24. Suzuki R, Takizawa T, Kuwata Y, et al. Effective anti-tumor activity of oxaliplatin encapsulated in transferrin-PEG-liposome. *Int J Pharm*. 2008;346(1):143–150. doi:10.1016/j.ijpharm.2007.06.010
25. Zhang N, Li C, Zhou D, et al. Cyclic RGD functionalized liposomes encapsulating urokinase for thrombolysis. *Acta Biomaterialia*. 2018;70:227–236. doi:10.1016/j.actbio.2018.01.038
26. Nie S. Understanding and overcoming major barriers in cancer nanomedicine. *Nanomedicine*. 2010;5(4):523–528. doi:10.2217/nmm.10.23
27. Biswas S, Deshpande PP, Perche F, Dodwadkar NS, Sane SD, Torchilin VP. Octa-arginine-modified pegylated liposomal doxorubicin: an effective treatment strategy for non-small cell lung cancer. *Cancer Lett*. 2013;335(1):191–200. doi:10.1016/j.canlet.2013.02.020
28. Jiang T, Zhang Z, Zhang Y, et al. Dual-functional liposomes based on pH-responsive cell-penetrating peptide and hyaluronic acid for tumor-targeted anticancer drug delivery. *Biomaterials*. 2012;33(36):9246–9258. doi:10.1016/j.biomaterials.2012.09.027
29. Moret F, Scheglmann D, Reddi E. Folate-targeted PEGylated liposomes improve the selectivity of PDT with meta-tetra(hydroxyphenyl)chlorin (m-THPC). *Photochem Photobiol Sci*. 2013;12(5):823–834. doi:10.1039/C3PP25384H
30. Sun M, Wang Y, Shen J, Xiao Y, Su Z, Ping Q. Octeotide-modification enhances the delivery and targeting of doxorubicin-loaded liposomes to somatostatin receptors expressing tumor in vitro and in vivo. *Nanotechnology*. 2010;21(47):475101. doi:10.1088/0957-4484/21/47/475101
31. Sahu BP, Baishya R, Hatiboruah JL, Laloo D, Biswas N. A comprehensive review on different approaches for tumor targeting using nanocarriers and recent developments with special focus on multifunctional approaches. *J Pharm Investig*. 2022;52(5):539–585. doi:10.1007/s40005-022-00583-x
32. LeBeau AM, Duriseti S, Murphy ST, et al. Targeting uPAR with antagonistic recombinant human antibodies in aggressive breast cancer. *Cancer Res*. 2013;73(7):2070. doi:10.1158/0008-5472.CAN-12-3526
33. Wu J, Liu Q, Lee RJ. A folate receptor-targeted liposomal formulation for paclitaxel. *Int J Pharm*. 2006;316(1):148–153. doi:10.1016/j.ijpharm.2006.02.027
34. Shim G, Jeong S, Oh JL, Kang Y. Lipid-based nanoparticles for photosensitive drug delivery systems. *J Pharm Investig*. 2022;52(2):151–160. doi:10.1007/s40005-021-00553-9
35. Farokhzad OC, Langer R. Impact of nanotechnology on drug delivery. *ACS Nano*. 2009;3(1):16–20. doi:10.1021/nn900002m
36. Ferrari M. Cancer nanotechnology: opportunities and challenges. *Nat Rev Cancer*. 2005;5(3):161–171. doi:10.1038/nrc1566
37. Gabizon A, Horowitz AT, Goren D, Tzemach D, Shmeeda H, Zalipsky S. In vivo fate of folate-targeted polyethylene-glycol liposomes in tumor-bearing mice. *Clin Cancer Res*. 2003;9(17):6551.
38. Saw PE, Park J, Lee E, et al. Effect of PEG pairing on the efficiency of cancer-targeting liposomes. *Theranostics*. 2015;5(7):746–754. doi:10.7150/thno.10732
39. Stefanick JF, Ashley JD, Kiziltepe T, Bilgicir B. A systematic analysis of peptide linker length and liposomal polyethylene glycol coating on cellular uptake of peptide-targeted liposomes. *ACS Nano*. 2013;7(4):2935–2947. doi:10.1021/nn305663e
40. Kirpotin D, Park JW, Hong K, et al. Sterically stabilized anti-HER2 immunoliposomes: design and targeting to human breast cancer cells in vitro. *Biochemistry*. 1997;36(1):66–75. doi:10.1021/bi962148u
41. Sapra P, Tyagi P, Allen TM. Ligand-targeted liposomes for cancer treatment. *Curr Drug Deliv*. 2005;2(4):369–381. doi:10.2174/156720105774370159
42. Yamada A, Taniguchi Y, Kawano K, Honda T, Hattori Y, Maitani Y. Design of folate-linked liposomal doxorubicin to its antitumor effect in mice. *Clin Cancer Res*. 2008;14(24):8161. doi:10.1158/1078-0432.CCR-08-0159
43. Bakhtiar A, Liew QX, Ng KY, Chowdhury EH. Active targeting via ligand-anchored pH-responsive strontium nanoparticles for efficient nucleic acid delivery into breast cancer cells. *J Pharm Investig*. 2022;52(2):243–257. doi:10.1007/s40005-022-00559-x
44. Lu Y, Low PS. Folate-mediated delivery of macromolecular anticancer therapeutic agents. *Adv Drug Deliv Rev*. 2012;64:342–352. doi:10.1016/j.addr.2012.09.020
45. Marshalek JP, Sheeran PS, Ingram P, Dayton PA, Witte RS, Matsunaga TO. Intracellular delivery and ultrasonic activation of folate receptor-targeted phase-change contrast agents in breast cancer cells in vitro. *J Control Release*. 2016;243:69–77. doi:10.1016/j.jconrel.2016.09.010
46. Muralidharan R, Babu A, Amreddy N, et al. Folate receptor-targeted nanoparticle delivery of HuR-RNAi suppresses lung cancer cell proliferation and migration. *J Nanobiotechnology*. 2016;14(1):47. doi:10.1186/s12951-016-0201-1
47. Siwowska K, Schmid RM, Cohrs S, Schibli R, Müller C. Folate receptor-positive gynecological cancer cells: in vitro and in vivo characterization. *Pharmaceutics*. 2017;10(3):72. doi:10.3390/ph10030072

48. Mirzaghavami PS, Khoei S, Khoei S, Shirvalilou S. Folic acid-conjugated magnetic triblock copolymer nanoparticles for dual targeted delivery of 5-fluorouracil to colon cancer cells. *Cancer Nanotechnol.* 2022;13(1):12. doi:10.1186/s12645-022-00120-3
49. Chango A, Emery-Fillon N, de Courcy GP, et al. A polymorphism (80G->A) in the reduced folate carrier gene and its associations with folate status and homocysteinemia. *Mol Genet Metab.* 2000;70(4):310–315. doi:10.1006/mgme.2000.3034
50. Wang S, Low PS. Folate-mediated targeting of antineoplastic drugs, imaging agents, and nucleic acids to cancer cells. *J Control Release.* 1998;53(1):39–48. doi:10.1016/S0168-3659(97)00236-8
51. Chen Y, Minh LV, Liu J, et al. Baicalin loaded in folate-PEG modified liposomes for enhanced stability and tumor targeting. *Colloids Surf B Biointerfaces.* 2016;140:74–82. doi:10.1016/j.colsurfb.2015.11.018
52. Nho TDT, Ly HT, Vo TS, et al. Enhanced anticancer efficacy and tumor targeting through folate-PEG modified nanoliposome loaded with 5-fluorouracil. *Adv Nat Sci Nanosci Nanotechnol.* 2017;8(1):015008.
53. Gabizon A, Horowitz AT, Goren D, et al. Targeting folate receptor with folate linked to extremities of poly(ethylene glycol)-grafted liposomes: in vitro studies. *Bioconjug Chem.* 1999;10(2):289–298. doi:10.1021/bc9801124
54. Kawano K, Maitani Y. Effects of polyethylene glycol spacer length and ligand density on folate receptor targeting of liposomal Doxorubicin in vitro. *J Drug Deliv.* 2011;2011:1–6. doi:10.1155/2011/160967
55. Riviere K, Huang Z, Jerger K, Macaraeg N, Szoka FC. Antitumor effect of folate-targeted liposomal doxorubicin in KB tumor-bearing mice after intravenous administration. *J Drug Target.* 2011;19(1):14–24. doi:10.3109/10611861003733953
56. Gabizon A, Shmeeda H, Horowitz AT, Zalipsky S. Tumor cell targeting of liposome-entrapped drugs with phospholipid-anchored folic acid-PEG conjugates. *Adv Drug Deliv Rev.* 2004;56(8):1177–1192. doi:10.1016/j.addr.2004.01.011
57. Qu M-H, Zeng R-F, Fang S, Dai Q-S, Li H-P, Long J-T. Liposome-based co-delivery of siRNA and docetaxel for the synergistic treatment of lung cancer. *Int J Pharm.* 2014;474(1):112–122. doi:10.1016/j.ijpharm.2014.08.019
58. Park JY, Shin Y, Won WR, et al. Development of AE147 peptide-conjugated nanocarriers for targeting uPAR-overexpressing cancer cells. *Int J Nanomedicine.* 2021;16:5437. doi:10.2147/IJN.S315619
59. Zucker D, Marcus D, Barenholz Y, Goldblum A. Liposome drugs' loading efficiency: a working model based on loading conditions and drug's physicochemical properties. *J Control Release.* 2009;139(1):73–80. doi:10.1016/j.jconrel.2009.05.036
60. Yuan M, Qiu Y, Zhang L, Gao H, He Q. Targeted delivery of transferrin and TAT co-modified liposomes encapsulating both paclitaxel and doxorubicin for melanoma. *Drug Deliv.* 2016;23(4):1171–1183. doi:10.3109/10717544.2015.1040527
61. Park EJ, Jun HW, Na IH, et al. CD48-expressing non-small-cell lung cancer cells are susceptible to natural killer cell-mediated cytotoxicity. *Arch Pharm Res.* 2022;45(1):1–10. doi:10.1007/s12272-021-01365-z
62. Hwang D, Dismuke T, Tikunov A, et al. Poly(2-oxazoline) nanoparticle delivery enhances the therapeutic potential of vismodegib for medulloblastoma by improving CNS pharmacokinetics and reducing systemic toxicity. *Nanomedicine.* 2021;32:102345. doi:10.1016/j.nano.2020.102345
63. Epps DE, Raub TJ, Caiolfa V, Chiari A, Zamai M. Determination of the affinity of drugs toward serum albumin by measurement of the quenching of the intrinsic tryptophan fluorescence of the protein. *J Pharm Pharmacol.* 1999;51(1):41–48. doi:10.1211/0022357991772079
64. Wang F, Yu R, Wen S, et al. Overexpressing microRNA-203 alleviates myocardial infarction via interacting with long non-coding RNA MIAT and mitochondrial coupling factor 6. *Arch Pharm Res.* 2021;44(5):525–535. doi:10.1007/s12272-021-01324-8
65. Nam S, Na HG, Oh EH, et al. Discovery and synthesis of 1,2,4-oxadiazole derivatives as novel inhibitors of Zika, dengue, Japanese encephalitis, and classical swine fever virus infections. *Arch Pharm Res.* 2022;45(4):280–293. doi:10.1007/s12272-022-01380-8
66. Lee S, Pham D-V, Park P-H. Sestrin2 induction contributes to anti-inflammatory responses and cell survival by globular adiponectin in macrophages. *Arch Pharm Res.* 2022;45(1):38–50. doi:10.1007/s12272-021-01364-0
67. Dos Santos N, Allen C, Doppen A-M, et al. Influence of poly(ethylene glycol) grafting density and polymer length on liposomes: relating plasma circulation lifetimes to protein binding. *Biochimica et Biophysica Acta.* 2007;1768(6):1367–1377. doi:10.1016/j.bbmem.2006.12.013
68. Bulbake U, Doppalapudi S, Kommineni N, Khan W. Liposomal formulations in clinical use: an updated review. *Pharmaceutics.* 2017;9(2):12. doi:10.3390/pharmaceutics9020012
69. Hattori Y, Maitani Y. Enhanced in vitro DNA transfection efficiency by novel folate-linked nanoparticles in human prostate cancer and oral cancer. *J Control Release.* 2004;97(1):173–183. doi:10.1016/j.jconrel.2004.03.007
70. Ohguchi Y, Kawano K, Hattori Y, Maitani Y. Selective delivery of folate-PEG-linked, nanoemulsion-loaded aclacinomycin A to KB nasopharyngeal cells and xenograft: effect of chain length and amount of folate-PEG linker. *J Drug Target.* 2008;16(9):660–667. doi:10.1080/10611860802201464
71. Shiokawa T, Hattori Y, Kawano K, et al. Effect of polyethylene glycol linker chain length of folate-linked microemulsions loading aclacinomycin A on targeting ability and antitumor effect in vitro and in vivo. *Clin Cancer Res.* 2005;11(5):2018. doi:10.1158/1078-0432.CCR-04-1129
72. Hinrichs WLJ, Manceño FA, Sanders NN, et al. The choice of a suitable oligosaccharide to prevent aggregation of PEGylated nanoparticles during freeze thawing and freeze drying. *Int J Pharm.* 2006;311(1):237–244. doi:10.1016/j.ijpharm.2005.12.032
73. Xiang G, Wu J, Lu Y, Liu Z, Lee RJ. Synthesis and evaluation of a novel ligand for folate-mediated targeting liposomes. *Int J Pharm.* 2008;356(1):29–36. doi:10.1016/j.ijpharm.2007.12.030
74. Fang C, Shi B, Pei Y-Y. Effect of MePEG molecular weight and particle size on in vitro release of tumor necrosis factor- α -loaded nanoparticles. *Acta Pharmacol Sin.* 2005;26(2):242–249. doi:10.1111/j.1745-7254.2005.00537.x
75. Kim J-Y, Kim J-K, Park J-S, Byun Y, Kim C-K. The use of PEGylated liposomes to prolong circulation lifetimes of tissue plasminogen activator. *Biomaterials.* 2009;30(29):5751–5756. doi:10.1016/j.biomaterials.2009.07.021
76. Shmeeda H, Mak L, Tzemach D, Astrahan P, Tarshish M, Gabizon A. Intracellular uptake and intracavitary targeting of folate-conjugated liposomes in a mouse lymphoma model with up-regulated folate receptors. *Mol Cancer Ther.* 2006;5(4):818–824. doi:10.1158/1535-7163.MCT-05-0543
77. Wang F, Xiao W, Elbahnasawy MA, et al. Optimization of the linker length of mannose-cholesterol conjugates for enhanced mRNA delivery to dendritic cells by liposomes. *Front Pharmacol.* 2018;9:980. doi:10.3389/fphar.2018.00980
78. Xing H, Li J, Xu W, et al. The effects of spacer length and composition on aptamer-mediated cell-specific targeting with nanoscale PEGylated liposomal doxorubicin. *Chembiochem.* 2016;17(12):1111–1117. doi:10.1002/cbic.201600092
79. Cavalli S, Tipton AR, Overhand M, Kros A. The chemical modification of liposome surfaces via a copper-mediated [3 + 2] azide-alkyne cycloaddition monitored by a colorimetric assay. *Chem Comm.* 2006;30:3193–3195. doi:10.1039/B606930D

80. Kumar A, Erasquin UJ, Qin G, Li K, Cai C. "Clickable", polymerized liposomes as a versatile and stable platform for rapid optimization of their peripheral compositions. *Chem Comm.* 2010;46(31):5746–5748. doi:10.1039/C0CC00784F
81. Feldborg LN, Jøelck RI, Andresen TL. Quantitative evaluation of bioorthogonal chemistries for surface functionalization of nanoparticles. *Bioconjug Chem.* 2012;23(12):2444–2450. doi:10.1021/bc3005057
82. Kang MH, Yoo HJ, Kwon YH, et al. Design of multifunctional liposomal nanocarriers for folate receptor-specific intracellular drug delivery. *Mol Pharm.* 2015;12(12):4200–4213. doi:10.1021/acs.molpharmaceut.5b00399

International Journal of Nanomedicine

Dovepress

Publish your work in this journal

The International Journal of Nanomedicine is an international, peer-reviewed journal focusing on the application of nanotechnology in diagnostics, therapeutics, and drug delivery systems throughout the biomedical field. This journal is indexed on PubMed Central, MedLine, CAS, SciSearch®, Current Contents®/Clinical Medicine, Journal Citation Reports/Science Edition, EMBase, Scopus and the Elsevier Bibliographic databases. The manuscript management system is completely online and includes a very quick and fair peer-review system, which is all easy to use. Visit <http://www.dovepress.com/testimonials.php> to read real quotes from published authors.

Submit your manuscript here: <https://www.dovepress.com/international-journal-of-nanomedicine-journal>